



# Homogenization of a conductive and radiative heat transfer problem

Grégoire Allaire, K. El Ganaoui

## ► To cite this version:

Grégoire Allaire, K. El Ganaoui. Homogenization of a conductive and radiative heat transfer problem. Multiscale Modeling and Simulation: A SIAM Interdisciplinary Journal, 2009, 7 (3), pp.1148-1170. 10.1137/080714737 . hal-00784061

**HAL Id: hal-00784061**

**<https://inria.hal.science/hal-00784061>**

Submitted on 4 Aug 2020

**HAL** is a multi-disciplinary open access archive for the deposit and dissemination of scientific research documents, whether they are published or not. The documents may come from teaching and research institutions in France or abroad, or from public or private research centers.

L'archive ouverte pluridisciplinaire **HAL**, est destinée au dépôt et à la diffusion de documents scientifiques de niveau recherche, publiés ou non, émanant des établissements d'enseignement et de recherche français ou étrangers, des laboratoires publics ou privés.

**ECOLE POLYTECHNIQUE**

**CENTRE DE MATHÉMATIQUES APPLIQUÉES**

*UMR CNRS 7641*

---

91128 PALAISEAU CEDEX (FRANCE). Tél: 01 69 33 46 00. Fax: 01 69 33 46 46  
<http://www.cmap.polytechnique.fr/>

**Homogenization of a conductive  
and radiative heat transfer  
problem**

Grégoire Allaire, Karima El Ganaoui

**R.I. 639**

*September 2008*



# HOMOGENIZATION OF A CONDUCTIVE AND RADIATIVE HEAT TRANSFER PROBLEM\*

GRÉGOIRE ALLAIRE <sup>†</sup> AND KARIMA EL GANAOU <sup>‡</sup>

**Abstract.** This paper is devoted to the homogenization of a heat conduction problem in a periodically perforated domain with a nonlinear and nonlocal boundary condition modeling radiative heat transfer in the perforations. Because of the considered critical scaling it is essential to use a method of two-scale asymptotic expansions inside the variational formulation of the problem. We obtain a nonlinear homogenized problem of heat conduction with effective coefficients which are computed via a cell problem featuring a radiative heat transfer boundary condition. We rigorously justify this homogenization process for the linearized problem by using two-scale convergence. We perform numerical simulations in 2-d: we reconstruct an approximate temperature field by adding to the homogenized temperature a corrector term. The computed numerical errors agree with the theoretical predicted errors and prove the effectiveness of our method for multiscale simulation of conductive and radiative heat transfer problems in periodically perforated domains.

**Key words.** Homogenization, two-scale convergence, radiative transfer, heat conduction.

**AMS subject classifications.**

**1. Introduction.** The goal of this paper is to theoretically and numerically study the homogenization of a conductive and radiative heat transfer problem in a perforated periodic media. The motivation of this problem comes from the nuclear reactor industry: an alternative concept to the usual pressurized water reactors is that of gas cooled reactors. Typically, a graphite matrix (playing the role of neutron moderator) is periodically perforated by long channels containing either the uranium fuel or a gas coolant which is helium. Recall that the fission nuclear reactions produce a large amount of heat which should be removed from the reactor core by a coolant in order to activate a steam generator (through a heat exchanger) and finally to produce electricity. Here we focus only on the heat transfer problem in such an heterogeneous medium. To simplify the exposition, we assume that the graphite and uranium matrix is already homogenized and can be considered as a single homogeneous material. Inside this matrix heat is transmitted by simple linear conduction. On the other hand, the helium heat conductivity is completely negligible with respect to the radiative transfer taking place inside the channels. We therefore face a coupled problem of heat conduction and radiation where the number of helium channels is very large, typically of the order of  $10^4$ . For dimensioning purposes as well as safety studies many numerical simulations have to be performed for which a direct approach (meshing all the geometric details) is impossible, or at least much too costly. Therefore, homogenization is a necessary ingredient for the study of such devices.

In this problem the goal of homogenization is twofold: first, it must yield a clear definition of what is the homogenized problem, and second, it has to give explicit formulas for the effective parameters as well as a recipe to approximate the exact solution. Indeed, since the original model is a mixture of two different type of equations (conduction and radiative transfer), the precise form of the homogenized system is not clear *a priori*. Concerning the second point, the original problem is posed in a perforated medium while the homogenized problem is posed in a homogeneous

---

\*This work has been supported by the French Atomic Energy Commission, DEN/DM2S at CEA Saclay.

<sup>†</sup>CMAP, ([gregoire.allaire@polytechnique.fr](mailto:gregoire.allaire@polytechnique.fr)).

<sup>‡</sup>CMAP, ([ganaoui@cmmap.polytechnique.fr](mailto:ganaoui@cmmap.polytechnique.fr)).

medium, so taking into account corrector terms is of paramount importance if one wants a geometrically sound reconstruction of an approximate solution.

Let us come back to the physical modeling of the original problem. The true problem is three-dimensional but the helium channels are long parallel tubes, so homogenization takes place only in the cross section. Therefore, it is not a severe restriction to consider only the two-dimensional homogenization of a cross section of the geometry (see Figure 2.1) as we shall do below. As usual in homogenization we denote by  $\varepsilon$  the period. The matrix perforated domain is  $\Omega_\varepsilon$  where energy transfer is done by conduction. The tubes or holes are  $\tau_{\varepsilon,i}$ , with boundaries  $\Gamma_{\varepsilon,i}$  which are grey-diffuse surfaces, and are filled by helium, assumed to be a transparent media without heat conduction nor absorption of radiation. Under these assumptions, the radiation equation can be integrated inside each hole  $\tau_{\varepsilon,i}$  to produce a complicated (non linear and non local) boundary condition on the wall  $\Gamma_{\varepsilon,i}$ . Section 2.2 gives a precise description of this boundary condition. Let us simply give the complete model when the emissivity is equal to one. For given bulk and surface heat source terms  $f$  and  $g$ , the temperature  $T_\varepsilon$  is a solution of

$$\left\{ \begin{array}{ll} -\operatorname{div}(K_\varepsilon \nabla T_\varepsilon) &= f \quad \text{in } \Omega_\varepsilon, \\ K_\varepsilon \nabla T_\varepsilon \cdot n &= g \quad \text{on } \partial\Omega, \\ -K_\varepsilon \nabla T_\varepsilon \cdot n &= \frac{\sigma}{\varepsilon} \left( T_\varepsilon^4(x) - \int_{\Gamma_{\varepsilon,i}} F(x,s) T_\varepsilon^4(s) d\gamma(s) \right) \quad \text{on } \Gamma_{\varepsilon,i}, \end{array} \right. \quad (1.1)$$

where  $F(x,s)$  is the so-called view factor for the wall  $\Gamma_{\varepsilon,i}$ . The scaling  $\varepsilon^{-1}$  in the right hand side of the boundary condition yields a perfect balance, in the limit as  $\varepsilon$  goes to zero, between the bulk heat conduction and the surface radiative transfer. A different scaling was studied in [7].

Since the seminal paper [12] it is known that the use of two-scale asymptotic expansions in perforated domains is sometimes delicate, especially when the boundary conditions are non linear and non local as here. Indeed, the homogenization of (1.1) by the formal method of two-scale asymptotic expansions (as presented in [8], [9], [11], [21]) is not completely obvious, all the more if one works with the strong form of the equations. As explained in Section 3 it is much simpler to perform the two-scale asymptotic expansions in the variational formulation of (1.1), symmetrically in the unknown and in the test function (following an idea of J.-L. Lions [16]). As a result we obtain that the leading term  $T(x)$  in the ansatz of  $T_\varepsilon(x)$  is the solution of the following non linear homogenized problem

$$\left\{ \begin{array}{ll} -\operatorname{div}(K^*(T) \nabla T) &= \frac{\operatorname{mes}(Y^*)}{\operatorname{mes}(Y)} f \quad \text{in } \Omega, \\ K^*(T) \nabla T \cdot n &= g \quad \text{on } \partial\Omega, \end{array} \right. \quad (1.2)$$

where  $K^*(T)$  is the effective conductivity, depending on the macroscopic temperature  $T$ , and defined through a local cell problem (3.3) which is a linearized conductive and radiative transfer problem in the unit cell (see Proposition 3.1).

In Section 4 we give a rigorous justification of such an homogenization result for the linearized version of (1.1) (see Theorem 4.6). Our main tools are two-scale convergence [2], [20] and suitable Taylor expansions of the test function on each hole boundary  $\Gamma_{\varepsilon,i}$  in order to take advantage of the view factor properties.

Eventually Section 5 is concerned with numerical simulations for this problem. Following a classical idea in periodic homogenization, we approximate the solution  $T_\varepsilon$

of (1.1) by the two first terms of its ansatz, i.e., the homogenized solution  $T$  plus the so-called corrector term

$$T_\varepsilon(x) \approx T(x) + \varepsilon \sum_{i=1}^d \omega_i \left( T^3(x), \frac{x}{\varepsilon} \right) \frac{\partial T}{\partial x_i}(x), \quad (1.3)$$

where  $\omega_i$  are the solutions of the cell problems. Since  $T$  is defined in the full domain  $\Omega$  while  $T_\varepsilon$  is merely defined in the perforated domain  $\Omega_\varepsilon$ , the corrector term is crucial for a good approximation. We make comparisons between the exact solution  $T_\varepsilon$  (or, at least, a converged numerical approximation of it, when available) and the reconstruction (1.3). We obtain a numerical error estimate of the order of  $\varepsilon$  in  $L^2(\Omega)$ , as predicted by homogenization theory [9]. Of course, the gain in terms of CPU time and memory storage is enormous when using (1.3) instead of solving the exact problem (1.1) since the homogenized problem (1.2) requires only a coarse mesh. Note however that the cell problem must be solved for different values of the macroscopic temperature  $T$ . Finally let us mention that a slightly simpler model is studied in [6] and that more details can be found in [14].

**2. Setting of the problem.** The goal of this section is to define precisely the geometry of the perforated periodic medium, to introduce the model of conductive and radiative heat transfer problem and to give some notations.

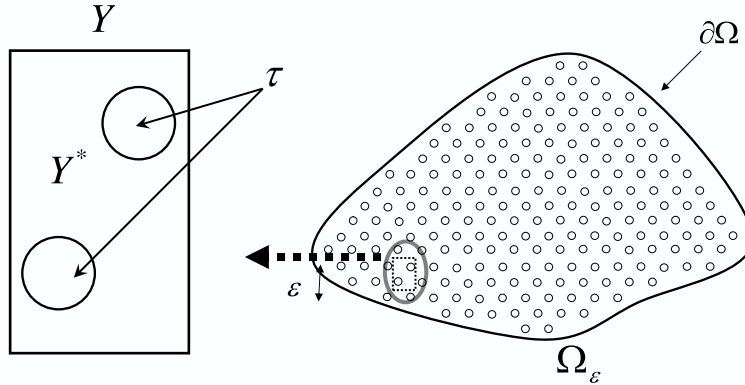


FIGURE 2.1. Reference cell and periodic domain

**2.1. Geometry.** Let  $\Omega$  be a smooth bounded open set in  $\mathbb{R}^d$  ( $d = 2$  or  $3$  in the applications). We define a periodic perforated domain  $\Omega_\varepsilon$ , where  $\varepsilon$  denotes its period, by removing from  $\Omega$  a collection of holes  $(\tau_{\varepsilon,k})_{k=1,\dots,M(\varepsilon)}$  in a periodic manner. Each hole  $\tau_\varepsilon^k$  is equal, up to a translation, to the same unit hole  $\tau$  rescaled at size  $\varepsilon$ . The domain  $\Omega$  is also subdivided in  $N(\varepsilon)$  periodicity cells  $(Y_{\varepsilon,i})_{i=1,\dots,N(\varepsilon)}$ , each of them being equal, up to a translation, to the same unit cell  $Y = \prod_{j=1}^d (0, \ell_j)$ . The number of periodicity cells is not equal to the number of holes since, in the application to gas cooled reactors, there are several holes per cell (see Figure 2.1). We denote by  $Y^*$  the

solid part of  $Y$ , i.e.,  $Y^* = Y \setminus \tau$ , and by  $\Gamma$  the boundary of  $\tau$  (by a slight abuse of language we denote by  $\tau$  an individual hole as well as all the holes contained in the unit cell  $Y$ ). To avoid some unnecessary technicalities (see [1] for details), we assume that, if a periodicity cell cuts the boundary of  $\Omega$ , then it does not contain any hole. The holes  $\tau_{\varepsilon,k}$  correspond to helium channels in our application where radiative heat transfer takes place, while  $\Omega_\varepsilon$  corresponds to the solid domain where conduction takes place. In summary we have

$$\Omega_\varepsilon = \Omega \setminus \bigcup_{k=1}^{M(\varepsilon)} \tau_{\varepsilon,k}, \quad \partial\Omega_\varepsilon = \partial\Omega \cup \Gamma_\varepsilon \quad \text{with} \quad \Gamma_\varepsilon = \bigcup_{k=1}^{M(\varepsilon)} \partial\tau_{\varepsilon,k} = \bigcup_{i=1}^{N(\varepsilon)} \Gamma_{\varepsilon,i}, \quad (2.1)$$

where  $\Gamma_{\varepsilon,i}$  denotes the boundaries of the holes  $\tau_{\varepsilon,k}$  inside the cell  $Y_{\varepsilon,i}$ . Denoting by  $\text{mes}$  the measure (surface or volume, depending on the context) of a set, we recall the following identities

$$\text{mes}(Y)\varepsilon^d = \frac{\text{mes}(\Omega)}{N(\varepsilon)}(1 + \mathcal{O}(\varepsilon)), \quad \text{mes}(\Gamma_{\varepsilon,i}) = \varepsilon^{d-1}\text{mes}(\Gamma), \quad \text{mes}(Y_{\varepsilon,i}) = \varepsilon^d \text{mes}(Y).$$

Denoting by  $d\gamma(x)$  the surface measure on  $\Gamma_\varepsilon$ , we define the center of mass  $x_{0,i}$  of  $\Gamma_{\varepsilon,i}$  by

$$x_{0,i} = \frac{1}{\text{mes}(\Gamma_{\varepsilon,i})} \int_{\Gamma_{\varepsilon,i}} x \, d\gamma(x) \quad \text{or equivalently} \quad \int_{\Gamma_{\varepsilon,i}} (x - x_{0,i}) d\gamma(x) = 0.$$

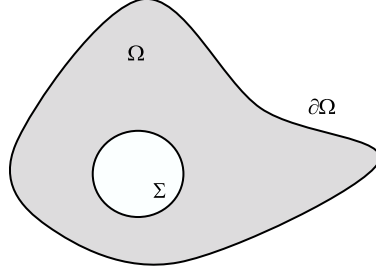
Similarly,  $y_0$  denotes the center of mass of the unit hole boundary  $\Gamma$ . We recall the following obvious identities.

LEMMA 2.1. *A smooth function  $f$  satisfies*

$$\begin{aligned} \int_{\Gamma_{\varepsilon,i}} f\left(\frac{x}{\varepsilon}\right) dx &= \varepsilon^{d-1} \int_{\Gamma} f(y) dy, \\ \int_{\Gamma_{\varepsilon,i}} f\left(\frac{x}{\varepsilon}\right) (x - x_{0,i}) dx &= \varepsilon^d \int_{\Gamma} f(y)(y - y_0) dy, \\ \int_{\Gamma_{\varepsilon,i}} f\left(\frac{x}{\varepsilon}\right) (x - x_{0,i}) \otimes (x - x_{0,i}) dx &= \varepsilon^{d+1} \int_{\Gamma} f(y)(y - y_0) \otimes (y - y_0) dy, \\ \varepsilon \sum_{i=1}^{N(\varepsilon)} \text{mes}(\Gamma_{\varepsilon,i}) f(x_{0,i}) &= \frac{\text{mes}(\Gamma)}{\text{mes}(Y)} \int_{\Omega} f(s) ds + \mathcal{O}(\varepsilon). \end{aligned}$$

**2.2. Boundary conditions.** As already said the holes are actually helium channels where radiative heat transfer takes place. Since helium is assumed to be transparent (no heat conduction nor absorption of radiation), this process is modeled by a boundary condition on the holes boundaries. Let us recall the modeling of radiative exchanges between grey-diffuse surfaces [15, 17]. A grey-diffuse surface emits and absorbs radiation in the same manner in all directions. Part of the received radiations can be reflected: a surface is thus characterized by its emissivity  $e$  which takes values between 0 (full reflection) and 1 (no reflection). Denoting by  $T$  the temperature and by  $R$  the radiosity, i.e. the intensity of emitted radiation, we have the following relationship

$$R(x) = e\sigma T^4(x) + (1 - e)J(x), \quad (2.2)$$

FIGURE 2.2. Domain with a radiative cavity  $\Sigma$ 

where  $\sigma$  is the Stefan-Boltzmann constant and  $J$  is given by

$$J(x) = \int_{\Sigma} F(x, s) R(s) d\gamma(s),$$

where  $F(x, s)$  is the view factor (a geometrical quantity) between two different points  $x$  and  $s$  of a cavity  $\Sigma$  (see Figure 2.2). Thus, the radiosity is given as the solution of an integral equation in terms of the temperature. For our application, the explicit formula of the view factor in 2-d for a convex cavity is

$$F(x, s) = \frac{n_s \cdot (x - s) n_x \cdot (s - x)}{2|s - x|^3}$$

where  $n_z$  denotes the unit normal at the point  $z$ . However, our mathematical study does not rely on this specific formula and we simply need the following properties of the kernel  $F$ : for any  $(x, s) \in \Sigma^2$ , it satisfies

- $F(x, s) \geq 0$ ,
- $F(x, s) = F(s, x)$ ,
- $\int_{\Sigma} F(x, s) ds = 1$ .

Let  $\mathfrak{J}$  be the operator going from  $L^p(\Sigma)$ ,  $1 \leq p \leq +\infty$ , into itself defined by

$$\mathfrak{J}(f)(x) = \int_{\Sigma} F(x, s) f(s) d\gamma(s). \quad (2.3)$$

Denoting by  $E$  the operator consisting of multiplying by the emissivity value  $e$ , (2.2) can be rewritten

$$R = (\text{Id} - (\text{Id} - E)\mathfrak{J})^{-1} E\sigma T^4.$$

On the cavity wall the energy balance reads

$$q - R + J = 0, \quad (2.4)$$

where  $q$  is the heat flux transmitted by conduction from the solid  $\Omega$  to the cavity  $\Sigma$ , from which we deduce

$$q = G(\sigma T^4),$$

where  $G$  is a linear non-local operator defined by

$$G(\varphi) = [\text{Id} - \mathfrak{J}] [\text{Id} - (\text{Id} - E)\mathfrak{J}]^{-1} E(\varphi) \quad \forall \varphi \in L^p(\Sigma). \quad (2.5)$$



Let us recall some properties of  $\mathfrak{J}$  defined by (2.3) (see [22]).

LEMMA 2.2. *The operator  $\mathfrak{J}$  going from  $L^p(\Sigma)$  to  $L^p(\Sigma)$ ,  $1 \leq p \leq \infty$ , satisfies*

- $\mathfrak{J}(c) = c$ ,  $\forall c \in \mathbb{R}$ ;
- $\|\mathfrak{J}\| \leq 1$ ;
- $\mathfrak{J}$  is non negative:  $\forall f \in L^p(\Sigma)$ ,  $f \geq 0 \Rightarrow \mathfrak{J}(f) \geq 0$ ;
- $\mathfrak{J}$  is symmetric (self-adjoint for  $p = 2$ ) in the sense that

$$\int_{\Sigma} \mathfrak{J}(\varphi)\psi = \int_{\Sigma} \mathfrak{J}(\psi)\varphi, \quad \forall \varphi \in L^p(\Sigma), \psi \in L^{p'}(\Sigma), \text{ with } \frac{1}{p} + \frac{1}{p'} = 1.$$

We easily deduce from Lemma 2.2 that  $(\text{Id} - \varsigma\mathfrak{J})$ ,  $0 \leq \varsigma < 1$ , is invertible (for  $\varsigma = 1$ ,  $(\text{Id} - \varsigma\mathfrak{J})$  is not invertible since  $\ker(\text{Id} - \mathfrak{J}) = \mathbb{R}$ ). In particular we deduce that  $G$  is well defined, symmetric and non negative (this is clear for  $0 < \varepsilon \leq 1$  and for  $\varepsilon = 0$  we find  $G \equiv 0$ ).

REMARK 2.3. *The operators defined by (2.3), (2.5) will be denoted by  $\mathfrak{J}_{\varepsilon}$ ,  $G_{\varepsilon}$  respectively, if acting on  $\Gamma_{\varepsilon}$  instead of  $\Gamma$ .*

**2.3. Governing equations.** Let  $K$  be the conductivity tensor of the unit cell  $Y^*$ . We assume  $K$  to be symmetric, uniformly coercive and bounded (in norm  $L^{\infty}$ ), i.e., there exist two positive constants  $0 < \alpha \leq \beta$  such that

$$\forall v \in \mathbb{R}^d, \text{ for a.e. } y \in Y^*, \quad \alpha|v|^2 \leq \sum_{i,j=1}^d K_{i,j}(y)v_i v_j \leq \beta|v|^2. \quad (2.6)$$

As usual,  $K(y)$  being a  $Y$ -periodic function, we define its  $Y_{\varepsilon}$ -periodic extension

$$K_{\varepsilon}(x) = K\left(\frac{x}{\varepsilon}\right).$$

For given bulk and surface source terms  $f$  and  $g$ , we consider the following mixed problem of conduction and radiative heat transfer for the unknown temperature  $T_{\varepsilon}$

$$\begin{cases} -\text{div}(K_{\varepsilon}\nabla T_{\varepsilon}) &= f & \text{in } \Omega_{\varepsilon}, \\ K_{\varepsilon}\nabla T_{\varepsilon} \cdot n &= g & \text{on } \partial\Omega, \\ -K_{\varepsilon}\nabla T_{\varepsilon} \cdot n &= \frac{1}{\varepsilon}G_{\varepsilon}(\sigma T_{\varepsilon}^4) & \text{on } \Gamma_{\varepsilon}, \end{cases} \quad (2.7)$$

where  $G$  is the operator defined by (2.5). For non-negative sources, the boundary value problem (2.7) admits a unique positive solution as was proved in [22]. The main difficulty in (2.7) is the non-linear and non-local boundary condition on  $\Gamma_{\varepsilon}$ . Note also the  $\varepsilon^{-1}$  scaling in the boundary condition which insures that the radiative condition will not disappear when passing to the limit  $\varepsilon \rightarrow 0$  and will be represented in the homogenized model.

**2.4. Notations.** The subscript  $\#$  in the definition of functional spaces on the unit cell  $Y$  indicates that we consider  $Y$ -periodic functions. We denote by  $L^2(\Omega; C_{\#}(Y))$  the space of measurable and square summable functions of  $x \in \Omega$  with values in the Banach space of continuous and  $Y$ -periodic functions of  $y$ . We denote by  $L^2(\Omega; H_{\#}^1(Y^*))$  the space of measurable and square summable functions of  $x \in \Omega$  with values in the Sobolev space  $H_{\#}^1(Y^*)$  of  $Y$ -periodic functions defined only on  $Y^*$ . We call cell-problem a problem that we solve only on the elementary cell of the periodic domain. Cell-problems usually take into account the microstructure behavior and contribute to the effective parameters calculation. We denote by  $\mathcal{O}(\varepsilon^p)$ ,  $p \in \mathbb{R}$  a function of  $\varepsilon > 0$  such that there exists a constant  $C$  not depending on  $\varepsilon$  so that we have  $|\mathcal{O}(\varepsilon^p)| \leq C\varepsilon^p$  for all  $\varepsilon > 0$ .

**3. Asymptotic expansions.** The mathematical theory of periodic homogenization is based on two-scale asymptotic analysis (see e.g. the books [3, 8, 9, 11, 21]). Two variables have to be considered: the macroscopic variable  $x$  and the microscopic one  $y$  with  $y = \frac{x}{\varepsilon}$ . The starting point of the heuristic method of two-scale asymptotic expansions is to assume that the solution  $T_\varepsilon$  of the problem to homogenize is given by the following series

$$T_\varepsilon(x) = \sum_{j=0}^{\infty} \varepsilon^j T_j \left( x, \frac{x}{\varepsilon} \right) \quad (3.1)$$

where each function  $T_j(x, y)$  is defined on  $\Omega \times Y$  and is  $Y$ -periodic with respect to  $y$ . The classical method of homogenization proceeds by injecting the ansatz (3.1) in the equations of the problem (i.e., in the strong formulation of the problem). It turns out that this approach fails here or is, at least, very difficult to properly achieve.

Indeed, the combination of the large scaling  $\varepsilon^{-1}$  and of the non-local character of the radiative boundary condition on the perforations makes the process of identifying successive powers of  $\varepsilon$  in the cascade of equations very involved, not to say tricky. Following an idea of J.-L. Lions [16], it is actually much safer to perform the two-scale asymptotic expansion in the variational formulation (i.e., in the weak form of the problem). In particular, the comparison between bulk and surface terms is much simpler and, the ansatz being symmetric between the unknown and tests function, it is enough to stop it at first order. Furthermore, working directly in the variational formulation allows us to take advantage of the symmetry properties of  $\mathfrak{J}$  and yields some (most welcome) geometrical simplifications.

Before we go into the numerous technical details, let us explain our main results obtained by applying this formal procedure. The homogenized problem for (2.7) is a non-linear conductivity equation in a continuous domain with a conductivity matrix depending on the temperature of the medium.

**PROPOSITION 3.1.** *The two first terms of the asymptotic expansion of the solution  $T_\varepsilon$  of (2.7) are given by*

$$T_\varepsilon(x) = T(x) + \varepsilon \sum_{i=1}^d \omega_i \left( T^3(x), \frac{x}{\varepsilon} \right) \frac{\partial T}{\partial x_i}(x) + \mathcal{O}(\varepsilon^2),$$

where  $T$  is the solution of the homogenized problem

$$\begin{cases} -\operatorname{div}(K^*(T)\nabla T) &= \frac{\operatorname{mes}(Y^*)}{\operatorname{mes}(Y)} f & \text{in } \Omega, \\ K^*(T)\nabla T \cdot n &= g & \text{on } \partial\Omega, \end{cases} \quad (3.2)$$

with an homogenized conductivity given by

$$K_{ij}^*(T) = \frac{1}{\operatorname{mes}(Y)} \left( \int_{Y^*} K(\nabla_y \omega_i + e_i) \cdot (\nabla_y \omega_j + e_j) + 4\sigma T^3 \int_{\Gamma} G(\omega_i + y_i)(\omega_j + y_j) \right),$$

and  $(\omega_i(T^3(x), y))_{1 \leq i \leq d}$  are the solutions of the cell problems

$$\begin{cases} -\operatorname{div}_y(K \nabla_y(e_i + \omega_i)) &= 0 & \text{in } Y^*, \\ -K \nabla_y(e_i + \omega_i) \cdot n &= 4\sigma T^3(x)G(\omega_i + y_i) & \text{on } \Gamma. \end{cases} \quad (3.3)$$

The homogenized problem (3.2) is a nonlinear conduction model with a conductivity matrix depending on the temperature. Radiative transfer is taken into account at the microstructure level in the cell problems which are conduction problems with a linearized radiative boundary condition on the wall of the holes.

The rigorous convergence of the homogenization process for the non linear model (2.7) is an open problem. Actually we are able to prove the convergence of  $T_\varepsilon$  to the homogenized temperature  $T$  only for a linearized version of (2.7) (see section 4). The main difficulty for the non linear model is that it lacks any property of convexity or of monotony (which are the usual simple assumptions required for homogenizing non linear problems). Another possibility would be to have at our disposal a comparison principle between two solutions which will be uniform in  $\varepsilon$ . Indeed, we know that a maximum principle applies to (2.7) (see [22]) but it seems delicate to obtain a comparison principle which is uniform in  $\varepsilon$  (at least we do not know how to proceed).

The rest of this section is devoted to the proof of proposition 3.1 which is divided in several subsections for the sake of clarity.

**3.1. Ansatz.** Because of the boundary conditions imposed on the perforations, the homogenization of the strong form (2.7) is not simple. Therefore, to obtain the homogenized problem for (2.7) we apply the formal two-scale asymptotic expansion method to its variational formulation

$$\begin{aligned} \int_{\Omega_\varepsilon} K_\varepsilon \nabla T_\varepsilon \cdot \nabla \varphi_\varepsilon + \frac{\sigma}{\varepsilon} \sum_{i=1}^{N(\varepsilon)} \int_{\Gamma_{\varepsilon,i}} (\text{Id} - \mathfrak{J}_\varepsilon)(\text{Id} - (\text{Id} - E)\mathfrak{J}_\varepsilon)^{-1} E \sigma T_\varepsilon^4 \varphi_\varepsilon = \\ = \int_{\Omega_\varepsilon} f \varphi_\varepsilon + \int_{\partial\Omega} g \varphi_\varepsilon. \end{aligned} \quad (3.4)$$

The boundary condition on  $\Gamma_\varepsilon$  is complicated since it requires the inversion of an operator. To avoid this inversion, we introduce two auxiliary variables  $\delta_\varepsilon$  and  $\chi_\varepsilon$  given by

$$\delta_\varepsilon = (\text{Id} - (\text{Id} - E)\mathfrak{J}_\varepsilon)^{-1} E(\sigma T_\varepsilon^4) \quad \text{and} \quad \chi_\varepsilon = (\text{Id} - (\text{Id} - E)\mathfrak{J}_\varepsilon)^{-1} \varphi_\varepsilon. \quad (3.5)$$

In particular, this implies that  $G(\sigma T_\varepsilon^4) = (\text{Id} - \mathfrak{J}_\varepsilon)\delta_\varepsilon$ . To simplify the writing we define on each boundary  $\Gamma_{\varepsilon,i}$  the operators  $A_\varepsilon$  and  $B_\varepsilon$ , going from  $L^p(\Gamma_{\varepsilon,i})$  into  $L^p(\Gamma_{\varepsilon,i})$ , by

$$A_\varepsilon = (\text{Id} - (\text{Id} - E)\mathfrak{J}_\varepsilon) \quad \text{and} \quad B_\varepsilon = (\text{Id} - \mathfrak{J}_\varepsilon)(\text{Id} - (\text{Id} - E)\mathfrak{J}_\varepsilon)$$

Then, the variational formulations of (2.7) and (3.5) are given by

$$\int_{\Omega_\varepsilon} K_\varepsilon \nabla T_\varepsilon \cdot \nabla \varphi_\varepsilon + \frac{1}{\varepsilon} \sum_{i=1}^{N(\varepsilon)} \int_{\Gamma_{\varepsilon,i}} B_\varepsilon \chi_\varepsilon \delta_\varepsilon = \int_{\Omega_\varepsilon} f \varphi_\varepsilon + \int_{\partial\Omega} g \varphi_\varepsilon, \quad (3.6)$$

$$\int_{\Gamma_{\varepsilon,i}} A_\varepsilon \delta_\varepsilon \psi_\varepsilon = e\sigma \int_{\Gamma_{\varepsilon,i}} T_\varepsilon^4 \psi_\varepsilon, \quad (3.7)$$

$$\int_{\Gamma_{\varepsilon,i}} A_\varepsilon \chi_\varepsilon \zeta_\varepsilon = \int_{\Gamma_{\varepsilon,i}} \varphi_\varepsilon \zeta_\varepsilon, \quad (3.8)$$

where  $\varphi_\varepsilon$ ,  $\psi_\varepsilon$  and  $\zeta_\varepsilon$  are test functions.

**REMARK 3.2.** Actually  $\chi_\varepsilon$  is not really an unknown of (2.7) since it depends solely on the test function  $\varphi_\varepsilon$ . However, introducing the supplementary test function  $\chi_\varepsilon$

allows us to keep a "symmetric" variational formulation where the unknowns  $(T_\varepsilon, \delta_\varepsilon)$  and the test functions  $(\varphi_\varepsilon, \chi_\varepsilon)$  play a symmetric role.

REMARK 3.3. The operators  $A$  and  $B$ , just defined, have similar properties to those of  $\mathfrak{J}$ . In particular, they are symmetric,  $A(c) = ec$  and  $B(c) = 0 \ \forall c \in \mathbb{R}$ ,  $A$  is invertible for  $0 < e \leq 1$ , and  $B$  is non negative.

**3.2. Homogenization results.** We first consider a two scale asymptotic expansion of the unknowns and the test functions

$$T_\varepsilon(x) = T(x) + \varepsilon T_1\left(x, \frac{x}{\varepsilon}\right) + \mathcal{O}(\varepsilon^2), \quad (3.9)$$

$$\delta_\varepsilon(x) = \delta\left(x, \frac{x}{\varepsilon}\right) + \varepsilon \delta_1\left(x, \frac{x}{\varepsilon}\right) + \mathcal{O}(\varepsilon^2), \quad (3.10)$$

$$\chi_\varepsilon(x) = \chi\left(x, \frac{x}{\varepsilon}\right) + \varepsilon \chi_1\left(x, \frac{x}{\varepsilon}\right) + \mathcal{O}(\varepsilon^2), \quad (3.11)$$

$$\varphi_\varepsilon(x) = \varphi(x) + \varepsilon \varphi_1\left(x, \frac{x}{\varepsilon}\right), \quad (3.12)$$

$$\psi_\varepsilon(x) = \psi\left(x, \frac{x}{\varepsilon}\right) + \varepsilon \psi_1\left(x, \frac{x}{\varepsilon}\right), \quad (3.13)$$

$$\zeta_\varepsilon(x) = \zeta\left(x, \frac{x}{\varepsilon}\right) + \varepsilon \zeta_1\left(x, \frac{x}{\varepsilon}\right). \quad (3.14)$$

We directly wrote  $T_0(x, y) = T(x)$  since we expect a macroscopic behavior of the temperature at its zero-th order. Then we perform a Taylor expansion of each quantity

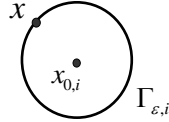


FIGURE 3.1. Example of 2D cavity with its center of mass  $x_{0,i}$

near the center of mass  $x_0$  of the considered cavity

$$\begin{aligned} T_\varepsilon^4(x) &= T^4(x_0) + 4T^3(x_0) \nabla T(x_0) \cdot (x - x_0) + \varepsilon 4T^3(x_0) T_1\left(x_0, \frac{x}{\varepsilon}\right) + \mathcal{O}(\varepsilon^2), \\ \delta_\varepsilon(x) &= \delta\left(x_0, \frac{x}{\varepsilon}\right) + \nabla_x \delta\left(x_0, \frac{x}{\varepsilon}\right) \cdot (x - x_0) + \varepsilon \delta_1\left(x_0, \frac{x}{\varepsilon}\right) + \mathcal{O}(\varepsilon^2), \\ \chi_\varepsilon(x) &= \chi\left(x_0, \frac{x}{\varepsilon}\right) + \nabla_x \chi\left(x_0, \frac{x}{\varepsilon}\right) \cdot (x - x_0) + \varepsilon \chi_1\left(x_0, \frac{x}{\varepsilon}\right) + \mathcal{O}(\varepsilon^2), \\ \varphi_\varepsilon(x) &= \varphi(x_0) + \nabla \varphi(x_0) \cdot (x - x_0) + \varepsilon \varphi_1\left(x_0, \frac{x}{\varepsilon}\right) + \mathcal{O}(\varepsilon^2), \\ \psi_\varepsilon(x) &= \psi\left(x_0, \frac{x}{\varepsilon}\right) + \nabla_x \psi\left(x_0, \frac{x}{\varepsilon}\right) \cdot (x - x_0) + \varepsilon \psi_1\left(x_0, \frac{x}{\varepsilon}\right) + \mathcal{O}(\varepsilon^2), \\ \zeta_\varepsilon(x) &= \zeta\left(x_0, \frac{x}{\varepsilon}\right) + \nabla_x \zeta\left(x_0, \frac{x}{\varepsilon}\right) \cdot (x - x_0) + \varepsilon \zeta_1\left(x_0, \frac{x}{\varepsilon}\right) + \mathcal{O}(\varepsilon^2) \end{aligned}$$

LEMMA 3.4. The first terms  $\delta$  and  $\chi$  of the asymptotic expansion (3.10) and (3.11) of  $\delta_\varepsilon$  and  $\chi_\varepsilon$ , respectively, are macroscopic in the following sense

$$\delta\left(x, \frac{x}{\varepsilon}\right) \equiv \delta(x) = \sigma T^4(x) \quad \text{and} \quad \chi\left(x, \frac{x}{\varepsilon}\right) \equiv \chi(x) = \frac{1}{e} \varphi(x),$$

where  $T$  and  $\varphi$  are the first terms of the asymptotic expansion of  $T_\varepsilon$  and  $\varphi_\varepsilon$ , respectively.

*Proof.* We inject the appropriate expansion in the variational formulation (3.7). Identifying its terms of order  $\varepsilon^0$  leads to

$$e\sigma \int_{\Gamma} T^4(x_0)\psi(x_0, y)dy = \int_{\Gamma} A\delta(x_0, y)\psi(x_0, y)dy,$$

which simply implies

$$A\delta(x_0, y) = e\sigma T^4(x_0) \quad \forall y \in \Gamma. \quad (3.15)$$

The operator  $A$  is coercive since  $0 < e \leq 1$  and  $\|\mathfrak{J}\| \leq 1$ . Thus (3.15) admits a unique solution. Since  $Ac = ec$  for any constant  $c \in \mathbb{R}$ , we deduce that the unique solution of (3.15) is  $\delta(x_0, y) = \sigma T^4(x_0)$ . In the same manner we can get the relationship between  $\chi$  and  $\varphi$ .  $\square$

Taking into account the results of lemma 3.4 we now obtain

LEMMA 3.5. *For any  $x$  in  $\Omega$ , the functions  $T$ ,  $T_1$  and  $\delta_1$  and  $\varphi$ ,  $\varphi_1$  and  $\chi_1$  are linked by the relationships*

$$A(\delta_1(x, y) + 4\sigma T^3(x)\nabla T(x) \cdot (y - y_0)) = 4e\sigma T^3(x)(T_1(x, y) + \nabla T(x) \cdot (y - y_0)) \quad (3.16)$$

and

$$A\left(\chi_1(x, y) + \frac{1}{e}\nabla\varphi(x) \cdot (y - y_0)\right) = \varphi_1(x, y) + \nabla\varphi(x) \cdot (y - y_0) \quad \forall x \in \Omega. \quad (3.17)$$

*Proof.* We consider the asymptotic expansions in the variational formulation (3.7). Thanks to the equality  $\delta = \sigma T^4$ , many terms disappear from both sides of (3.7). The  $\varepsilon$  order terms yield

$$\begin{aligned} & \int_{\Gamma} A(\delta_1(x_0, y) + 4\sigma T^3(x_0)\nabla T(x_0) \cdot (y - y_0))\psi(x_0, y)dy \\ &= 4e\sigma T^3(x_0) \int_{\Gamma_{\varepsilon, i}} (T_1(x_0, y) + \nabla T(x_0) \cdot (y - y_0))\psi(x_0, y)dy, \end{aligned} \quad (3.18)$$

which is precisely the variational formulation of (3.16). The same arguments applied to (3.8) lead to (3.17).  $\square$

We now consider the main variational formulation (3.4) corresponding to the boundary value problem (2.7). For the moment we simply focus on its more delicate term, involving the radiative boundary condition

$$\frac{1}{\varepsilon} \sum_{i=1}^{N(\varepsilon)} \int_{\Gamma_{\varepsilon, i}} B_{\varepsilon} \chi_{\varepsilon} \delta_{\varepsilon}.$$

For this term only we need to be a little bit more precise in our asymptotic expansions, pushing then to the second order in  $\varepsilon$ . The reader should not be afraid by this seemingly contradiction with our previous argument that first order ansatz are enough: actually the second order terms will disappear in the limit. Thus we replace (3.10) and (3.11) (after Taylor expansion) by

$$\begin{aligned} \chi_{\varepsilon}(x) &= \frac{1}{e}\varphi(x_0) + \frac{1}{e}\nabla\varphi(x_0) \cdot (x - x_0) + \varepsilon\chi_1\left(x_0, \frac{x}{\varepsilon}\right) + \varepsilon^2\tilde{\chi}_{2, \varepsilon}(x) + \mathcal{O}(\varepsilon^3), \\ \delta_{\varepsilon}(x) &= \sigma T^4(x_0) + 4\sigma T^3(x_0)\nabla T(x_0) \cdot (x - x_0) + \varepsilon\delta_1\left(x_0, \frac{x}{\varepsilon}\right) + \varepsilon^2\tilde{\delta}_{2, \varepsilon}(x) + \mathcal{O}(\varepsilon^3), \end{aligned}$$

where we do not give any details on the second-order terms  $\tilde{\chi}_{2,\varepsilon}$  and  $\tilde{\delta}_{2,\varepsilon}$  because they will disappear after this stage. We compute

$$\begin{aligned}
& B_\varepsilon \chi_\varepsilon \delta_\varepsilon = \\
& B_\varepsilon \frac{1}{\varepsilon} \varphi(x_0) \left[ \sigma T^4(x_0) + 4\sigma T^3(x_0) \nabla T(x_0) \cdot (x - x_0) + \varepsilon \delta_1 \left( x_0, \frac{x}{\varepsilon} \right) + \varepsilon^2 \tilde{\delta}_{2,\varepsilon}(x) \right] \\
& + B_\varepsilon \left( \frac{1}{\varepsilon} \nabla \varphi(x_0) \cdot (x - x_0) \right) \left[ \sigma T^4(x_0) + 4\sigma T^3(x_0) \nabla T(x_0) \cdot (x - x_0) + \varepsilon \delta_1 \left( x_0, \frac{x}{\varepsilon} \right) \right] \\
& + \varepsilon B_\varepsilon \chi_1 \left( x_0, \frac{x}{\varepsilon} \right) \left[ \sigma T^4(x_0) + 4\sigma T^3(x_0) \nabla T(x_0) \cdot (x - x_0) + \varepsilon \delta_1 \left( x_0, \frac{x}{\varepsilon} \right) \right] \\
& + \varepsilon^2 B_\varepsilon \tilde{\chi}_{2,\varepsilon}(x) \sigma T^4(x_0) + \mathcal{O}(\varepsilon^3).
\end{aligned} \tag{3.19}$$

Because  $B_\varepsilon$  is symmetric and its kernel is  $\mathbb{R}$  (the constants), the terms in (3.19) which contain  $\tilde{\chi}_2$  and  $\tilde{\delta}_2$  will disappear when integrating on  $\Gamma_{\varepsilon,i}$ . Remark also that, after integration and summation over all cells, we obtain a remainder term given by

$$\frac{1}{\varepsilon} \sum_{i=1}^{N(\varepsilon)} \text{mes}(\Gamma_{\varepsilon,i}) \mathcal{O}(\varepsilon^3) = \mathcal{O}(\varepsilon^{-d}) \mathcal{O}(\varepsilon^{d-1}) \mathcal{O}(\varepsilon^2) = \mathcal{O}(\varepsilon)$$

which can safely be neglected. Thus, integrating on  $\Gamma_{\varepsilon,i}$ , multiplying by  $\varepsilon^{-1}$ , summing on  $i$  and using lemma 2.1, we obtain the following limit

$$\begin{aligned}
& \frac{1}{\varepsilon} \sum_{i=1}^{N(\varepsilon)} \int_{\Gamma_{\varepsilon,i}} B_\varepsilon \chi_\varepsilon \delta_\varepsilon = \\
& \frac{1}{\text{mes}(Y)} \left[ \int_{\Omega} \int_{\Gamma} B \left( \frac{1}{\varepsilon} \nabla \varphi(x) \cdot (y - y_0) \right) 4\sigma T^3(x) \nabla T(x) \cdot (y - y_0) \, dy \, dx \right. \\
& + \int_{\Omega} \int_{\Gamma} B \frac{1}{\varepsilon} \nabla \varphi(x) \cdot (y - y_0) \delta_1(x, y) \, dy \, dx \\
& + \int_{\Omega} \int_{\Gamma} B \chi_1(x, y) 4\sigma T^3(x) \nabla T(x) \cdot (y - y_0) \, dy \, dx \\
& \left. + \int_{\Omega} \int_{\Gamma} B \chi_1(x, y) \delta_1(x, y) \, dy \, dx \right] + \mathcal{O}(\varepsilon).
\end{aligned} \tag{3.20}$$

It is much easier to pass to the limit in the other terms of the variational formulation (3.6) (so we skip the details) and we eventually obtain the following limit

$$\begin{aligned}
& \frac{1}{\text{mes}(Y)} \left[ \int_{\Omega} \int_{Y^*} K(y) (\nabla T(x) + \nabla_y T_1(x, y)) \cdot (\nabla \varphi(x) + \nabla_y \varphi_1(x, y)) \, dy \, dx \right. \\
& + \int_{\Omega} 4\sigma T^3(x) \int_{\Gamma} (\text{Id} - \mathfrak{J}) \frac{1}{\varepsilon} \nabla \varphi(x) \cdot (y - y_0) A [\nabla T(x) \cdot (y - y_0)] \, dy \, dx \\
& + \int_{\Omega} \int_{\Gamma} (\text{Id} - \mathfrak{J}) \frac{1}{\varepsilon} \nabla \varphi(x) \cdot (y - y_0) A \delta_1(x, y) \, dy \, dx \\
& + \int_{\Omega} \int_{\Gamma} (\text{Id} - \mathfrak{J}) \chi_1(x, y) A [4\sigma T^3(x) \nabla T(x) \cdot (y - y_0)] \, dy \, dx \\
& \left. + \int_{\Omega} \int_{\Gamma} (\text{Id} - \mathfrak{J}) \chi_1(x, y) A \delta_1(x, y) \, dy \, dx \right] \\
& = \frac{\text{mes}(Y^*)}{\text{mes}(Y)} \int_{\Omega} f \varphi \, dx + \int_{\partial\Omega} g \varphi \, d\gamma(x).
\end{aligned} \tag{3.21}$$

From (3.17) and the equality  $G = (\text{Id} - \mathfrak{J})A^{-1}$  we deduce

$$(\text{Id} - \mathfrak{J})\chi_1 = \frac{1}{e}G\varphi_1 + \frac{1}{e}G\nabla\varphi \cdot (y - y_0) - (\text{Id} - \mathfrak{J})\frac{1}{e}\nabla\varphi \cdot (y - y_0). \quad (3.22)$$

Now we substitute in (3.21) formula (3.16) for  $A\delta_1$  and formula (3.22) for  $(\text{Id} - \mathfrak{J})\chi_1$ . After some simplifications we obtain

$$\begin{aligned} & \frac{1}{\text{mes}(Y)} \left( \int_{\Omega} \int_{Y^*} K(y) (\nabla T(x) + \nabla_y T_1(x, y)) \cdot (\nabla\varphi(x) + \nabla_y\varphi_1(x, y)) \right. \\ & \quad \left. + 4\sigma \int_{\Omega} T^3(x) \int_{\Gamma} [\varphi_1(x, y) + \nabla\varphi(x) \cdot (y - y_0)] \right. \\ & \quad \left. G[T_1(x, y) + \nabla T(x) \cdot (y - y_0)] \right) \\ & = \frac{\text{mes}(Y^*)}{\text{mes}(Y)} \int_{\Omega} f(x)\varphi(x) + \int_{\partial\Omega} g(x)\varphi(x), \end{aligned} \quad (3.23)$$

which is just a variational formulation for the unknown  $(T, T_1)$  with a test function  $(\varphi, \varphi_1)$ .

Taking  $\varphi = 0$  in (3.23) yields the cell problem

$$\int_{\Omega} \int_{Y^*} K(\nabla T + \nabla_y T_1) \cdot \nabla_y \varphi_1 + 4\sigma \int_{\Omega} T^3 \int_{\Gamma} G\varphi_1 [T_1 + \nabla T \cdot (y - y_0)] = 0$$

which is the variational formulation of

$$\begin{cases} -\text{div}_y(K(\nabla T + \nabla_y T_1)) &= 0 & \text{in } Y^*, \\ -K(\nabla T + \nabla_y T_1) \cdot n &= 4\sigma T^3(x)G(T_1 + \nabla T \cdot (y - y_0)) & \text{on } \Gamma, \end{cases} \quad (3.24)$$

from which we deduce a formula for  $T_1$  in terms of  $T$

$$T_1(x, y) = \sum_{i=1}^d \omega_i(T^3(x), y) \frac{\partial T}{\partial x_i}(x). \quad (3.25)$$

Taking  $\varphi_1 = 0$  in (3.23) and using (3.25) yields the variational formulation of the homogenized problem (3.2) with the effective conductivity tensor as announced in proposition 3.1.

**4. Rigorous homogenization for a linear model.** In this section we give a rigorous homogenization result for the linearized version of (2.7) using two-scale convergence [2, 20]. To simplify further the exposition we focus on the case of so-called black walls, i.e., we assume that  $e = 1$ . It allows us to avoid the use of the additional unknowns  $\delta_\varepsilon$  and  $\chi_\varepsilon$ . However, our method can extend without further conceptual difficulty to the case  $0 < e < 1$ . Although the non-linear problem (2.7) admits a unique solution, it is not the case of its linearized version which admits a solution, unique up to the addition of a constant. Therefore, to ensure the uniqueness of the solution, we replace the Neumann condition on  $\partial\Omega$  by a Dirichlet one. In other words, we now consider

$$\begin{cases} -\text{div}(K_\varepsilon \nabla T_\varepsilon) &= f & \text{in } \Omega_\varepsilon, \\ T_\varepsilon &= 0 & \text{on } \partial\Omega, \\ -K_\varepsilon \nabla T_\varepsilon \cdot n &= \frac{1}{\varepsilon}(\text{Id} - \mathfrak{J}_\varepsilon)(\tilde{\sigma} T_\varepsilon) & \text{on } \Gamma_\varepsilon, \end{cases} \quad (4.1)$$

where  $\tilde{\sigma} = \sigma T_0^3$  with  $T_0$  a positive constant reference temperature. Recall that, since  $e = 1$ , we have  $G = (\text{Id} - \mathfrak{J})$ .

**4.1. Well-posedness and a priori estimates.** First we discuss the existence and uniqueness of the solution of (4.1), then we derive a priori estimates. The variational formulation of (4.1) is, for any  $\varphi_\varepsilon \in H^1(\Omega_\varepsilon)$  such that  $\varphi_\varepsilon = 0$  on  $\partial\Omega$ ,

$$\int_{\Omega_\varepsilon} K_\varepsilon \nabla T_\varepsilon \cdot \nabla \varphi_\varepsilon + \tilde{\sigma} \frac{1}{\varepsilon} \sum_k \int_{\Gamma_{\varepsilon,k}} (\text{Id} - \mathfrak{J}_\varepsilon)(\varphi_\varepsilon) T_\varepsilon = \int_{\Omega_\varepsilon} f \varphi_\varepsilon, \quad (4.2)$$

where we have used the symmetric character of  $(\text{Id} - \mathfrak{J}_\varepsilon)$ . The operator  $(\text{Id} - \mathfrak{J}_\varepsilon)$  is non-negative, so the linear problem (4.1) is coercive and has a unique solution in  $H^1(\Omega_\varepsilon)$  by application of the Lax-Milgram lemma.

We now recall a convenient extension lemma due to [12].

LEMMA 4.1. *There exists a continuous linear extension  $P_\varepsilon$  from  $H^1(\Omega_\varepsilon)$  to  $H^1(\Omega)$  such that*

$$\forall \varphi_\varepsilon \in H^1(\Omega_\varepsilon) \quad P_\varepsilon(\varphi_\varepsilon)|_{\Omega_\varepsilon} = \varphi_\varepsilon \quad (4.3)$$

and there exists a constant  $C > 0$ , which does not depend on  $\varepsilon$ , such that

$$\|P_\varepsilon(\varphi_\varepsilon)\|_{H^1(\Omega)} \leq C \|\varphi_\varepsilon\|_{H^1(\Omega_\varepsilon)} \quad \forall \varphi_\varepsilon \in H^1(\Omega_\varepsilon).$$

We also recall a classical lemma.

LEMMA 4.2. *There exists a constant  $C > 0$ , not depending on  $\varepsilon$ , such that*

$$\varepsilon^{1/2} \|\varphi_\varepsilon\|_{L^2(\Gamma_\varepsilon)} \leq C \|\varphi_\varepsilon\|_{H^1(\Omega_\varepsilon)} \quad \forall \varphi_\varepsilon \in H^1(\Omega_\varepsilon). \quad (4.4)$$

We are ready to give the *a priori* estimate.

PROPOSITION 4.3. *Let  $T_\varepsilon$  be the solution of (4.1) (extended to  $\Omega$ ). There exists a constant  $C$  independent on  $\varepsilon$  such that*

$$\|T_\varepsilon\|_{H^1(\Omega)} \leq C \quad (4.5)$$

and

$$\varepsilon \int_{\Gamma_\varepsilon} |T_\varepsilon(x)|^2 d\gamma_\varepsilon(x) \leq C. \quad (4.6)$$

*Proof.* Using the properties of the extension  $P_\varepsilon$  and the Poincaré inequality in  $\Omega$ , we easily find the estimate (4.5). Using lemma 4.2 and (4.5) we deduce (4.6).  $\square$

We finally recall the definition and main results of two-scale convergence [2, 20].

DEFINITION 4.4. *A bounded sequence  $u_\varepsilon$  in  $L^2(\Omega)$  is said to two-scale converge to a function  $u_0(x, y) \in L^2(\Omega \times Y)$  if there exists a subsequence still denoted by  $u_\varepsilon$  such that*

$$\lim_{\varepsilon \rightarrow 0} \int_{\Omega} u_\varepsilon(x) \psi\left(x, \frac{x}{\varepsilon}\right) dx = \frac{1}{\text{mes}(Y)} \int_{\Omega} \int_Y u_0(x, y) \psi(x, y) dx dy \quad (4.7)$$

for any  $Y$ -periodic test function  $\psi(x, y) \in L^2(\Omega; C_\#(Y))$ .

A notion of two-scale convergence on periodic surfaces was also introduced in [5, 19]. We recall its necessary results.

PROPOSITION 4.5. *Let  $u_\varepsilon$  be a sequence of  $L^2(\Gamma_\varepsilon)$  such that*

$$\varepsilon \int_{\Gamma_\varepsilon} |u_\varepsilon(x)|^2 d\gamma_\varepsilon(x) \leq C. \quad (4.8)$$



There exists a subsequence, still denoted by  $u_\varepsilon$  and a function  $u_0 \in L^2(\Omega; L^2(\Gamma))$  such that  $u_\varepsilon(x)$  two-scale converge to  $u_0(x, y)$  in the following sense

$$\lim_{\varepsilon \rightarrow 0} \varepsilon \int_{\Gamma_\varepsilon} u_\varepsilon(x) \psi\left(x, \frac{x}{\varepsilon}\right) dx = \frac{1}{\text{mes}(Y)} \int_{\Omega} \int_{\Gamma} u_0(x, y) \psi(x, y) dx d\gamma(y) \quad (4.9)$$

for any  $Y$ -periodic test function  $\psi(x, y) \in L^2(\Omega; C_\#(Y))$ .

**4.2. Homogenization results in the linear case.** The method of two-scale asymptotic expansions, as explained for the non-linear case in section 3, can also be applied to the linear case. There are some slight differences in the results that we now briefly summarize. The homogenized problem is the following linear equation

$$\begin{cases} -\text{div}(K^* \nabla T) &= \frac{\text{mes}(Y^*)}{\text{mes}(Y)} f & \text{in } \Omega, \\ T &= 0 & \text{on } \partial\Omega, \end{cases} \quad (4.10)$$

where the homogenized conductivity is given by

$$K_{ij}^* = \frac{1}{\text{mes}(Y)} \int_{Y^*} K(\nabla_y \omega_i + e_i) \cdot (\nabla_y \omega_j + e_j) + \tilde{\sigma} \int_{\Gamma} (\text{Id} - \mathfrak{J})(\omega_i + y_i)(\omega_j + y_j), \quad (4.11)$$

and the cell problems are

$$\begin{cases} -\text{div}_y(K(e_i + \nabla_y \omega_i)) &= 0 & \text{in } Y^*, \\ -K(e_i + \nabla_y \omega_i) \cdot n &= \tilde{\sigma}(\text{Id} - \mathfrak{J})(\omega_i + y_i) & \text{on } \Gamma, \\ y &\mapsto \omega_i(y) & \text{is } Y\text{-periodic.} \end{cases} \quad (4.12)$$

Clearly, (4.10) admits a unique solution  $T \in H_0^1(\Omega)$  and (4.12) a unique solution  $\omega_i \in H_\#^1(Y^*)$ , up to an additive constant (which does not play any role in the sequel). We define a corrector function  $T_1(x, y) \in L^2(\Omega; H_\#^1(Y^*))$  by

$$T_1(x, y) = \sum_{i=1}^d \omega_i(y) \frac{\partial T}{\partial x_i}(x). \quad (4.13)$$

Our main result in this section is the following

**THEOREM 4.6.** *Let  $T_\varepsilon$  be the sequence of solutions of (4.1). Let  $T$  be the solution of the homogenized problem (4.10) and  $T_1$  be the function defined by (4.13). Then,  $T_\varepsilon$  and  $\nabla T_\varepsilon$ , extended to the entire domain  $\Omega$ , two-scale converge to  $T$  and  $\nabla_x T + \nabla_y T_1$ , respectively.*

*Proof.* The *a priori* estimate (4.5) implies that  $T_\varepsilon$  is bounded in  $H^1(\Omega)$ . Thus, we can extract a subsequence which converges weakly to a function  $T$  in  $H^1(\Omega)$  and, according to Proposition 1.14 in [2], the subsequence  $\nabla T_\varepsilon$  two-scale converges to  $\nabla T(x) + \nabla_y T_1(x, y)$  for some function  $T_1 \in L^2(\Omega; H_\#^1(Y))$ . Similarly, according to proposition 4.5, up to another subsequence,  $T_\varepsilon$  two-scale converges on the periodic surface  $\Gamma_\varepsilon$  to the limit  $T(x)$ .

In the variational formulation (4.2) we choose an oscillating test function  $\varphi_\varepsilon$  defined by

$$\varphi_\varepsilon(x) = \varphi(x) + \varepsilon \varphi_1\left(x, \frac{x}{\varepsilon}\right) \quad \text{with} \quad \varphi_1(x, y) = \sum_{i=1}^d \frac{\partial \varphi}{\partial x_i}(x) \omega_i(y)$$

where  $\varphi \in C_c^\infty(\Omega)$  and  $\omega_i$  are the solutions of cell problems (4.12). In order to evaluate  $(\text{Id} - \mathfrak{J}_\varepsilon)(\varphi_\varepsilon)$ , we write a Taylor expansion of  $\varphi_\varepsilon$  around  $x_{\varepsilon,k}$ , the center of mass of  $\Gamma_{\varepsilon,k}$ ,

$$\begin{aligned} \varphi_\varepsilon(x) &= \varphi(x_{\varepsilon,k}) + \nabla \varphi(x_{\varepsilon,k}) \cdot (x - x_{\varepsilon,k}) + \frac{1}{2} \nabla \nabla \varphi(x_{\varepsilon,k}) (x - x_{\varepsilon,k}) \cdot (x - x_{\varepsilon,k}) + \varepsilon \varphi_1\left(x_{\varepsilon,k}, \frac{x}{\varepsilon}\right) \\ &\quad + \varepsilon \nabla_x \varphi_1\left(x_{\varepsilon,k}, \frac{x}{\varepsilon}\right) \cdot (x - x_{\varepsilon,k}) + \mathcal{O}(\varepsilon^3). \end{aligned} \quad (4.14)$$

Remark that  $\nabla \varphi(x_{\varepsilon,k})$  is constant, so it can be factorized out when applying the operator  $\mathfrak{J}_\varepsilon$  to  $\varphi_\varepsilon$ . After applying  $\mathfrak{J}_\varepsilon$  to (4.14), in order to recover continuous functions we shall apply the following Taylor expansion

$$\frac{\partial \varphi}{\partial x_i}(x_{\varepsilon,k}) = \frac{\partial \varphi}{\partial x_i}(x) - \nabla \frac{\partial \varphi}{\partial x_i}(x) \cdot (x - x_{\varepsilon,k}) + \mathcal{O}(\varepsilon^2).$$

Therefore, we obtain

$$\frac{1}{\varepsilon} (\text{Id} - \mathfrak{J}_\varepsilon)(\varphi_\varepsilon)(x) = \varepsilon \left( \psi_{1,\varepsilon}(x) + \psi_{2,\varepsilon}(x) + \mathcal{O}(\varepsilon) \right)$$

with

$$\begin{aligned} \psi_{1,\varepsilon}(x) &= \frac{1}{\varepsilon} \sum_{i=1}^d (\text{Id} - \mathfrak{J}_\varepsilon) \left( \omega_i \left( \frac{x}{\varepsilon} \right) + \frac{x_i - x_{\varepsilon,k}^i}{\varepsilon} \right) \left( \frac{\partial \varphi}{\partial x_i}(x) - \nabla \frac{\partial \varphi}{\partial x_i}(x) \cdot (x - x_{\varepsilon,k}) \right), \\ \psi_{2,\varepsilon}(x) &= \frac{1}{\varepsilon^2} \left( \frac{1}{2} \nabla \nabla \varphi(x) (\text{Id} - \mathfrak{J}_\varepsilon) \left( (x - x_{\varepsilon,k}) \cdot (x - x_{\varepsilon,k}) \right) \right. \\ &\quad \left. + \varepsilon \sum_{i=1}^d \nabla \frac{\partial \varphi}{\partial x_i}(x) \cdot (\text{Id} - \mathfrak{J}_\varepsilon) \left( (x - x_{\varepsilon,k}) \omega_i \left( \frac{x}{\varepsilon} \right) \right) \right), \end{aligned}$$

where  $x_{\varepsilon,k}^i$  denotes the  $i^{\text{th}}$  component of  $x_{\varepsilon,k}$ . Remark that  $\psi_{2,\varepsilon}(x) = \psi_2\left(x, \frac{x}{\varepsilon}\right)$  so  $\psi_{2,\varepsilon}(x)$  two-scale converges to  $\psi_2(x, y)$  given by

$$\psi_2(x, y) = \frac{1}{2} \nabla \nabla \varphi(x) (\text{Id} - \mathfrak{J}) [(y - y_0) \cdot (y - y_0)] + \sum_{i=1}^d \nabla \frac{\partial \varphi}{\partial x_i}(x) \cdot (\text{Id} - \mathfrak{J}) [(y - y_0) \omega_i(y)].$$

By virtue of proposition 4.5 we have

$$\lim_{\varepsilon \rightarrow 0} \varepsilon \sum_{k=1}^{N(\varepsilon)} \int_{\Gamma_{\varepsilon,k}} \psi_{2,\varepsilon} T_\varepsilon = \frac{\text{mes}(\Gamma)}{\text{mes}(Y)} \int_{\Omega} T(x) \int_{\Gamma} \psi_2(x, y) dy \, dx = 0, \quad (4.15)$$

since

$$\int_{\Gamma} \psi_2(x, y) \, dy = 0.$$

Concerning the term containing  $\psi_{1,\varepsilon}$  we use the classical "compensated compactness" trick of  $H$ -convergence [18] which relies on a comparison with the variational formulation of the cell problems (4.12). More precisely, after rescaling (4.12) we have

$$\int_{\Gamma_\varepsilon} \tilde{\sigma} (\text{Id} - \mathfrak{J}_\varepsilon) \left( \omega_i \left( \frac{x}{\varepsilon} \right) + \frac{x_i}{\varepsilon} \right) \left( T \frac{\partial \varphi}{\partial x_i} \right) = -\varepsilon \int_{\Omega_\varepsilon} K_\varepsilon \nabla \left( \omega_i \left( \frac{x}{\varepsilon} \right) + \frac{x_i}{\varepsilon} \right) \cdot \nabla \left( T \frac{\partial \varphi}{\partial x_i} \right).$$

This implies that

$$\begin{aligned} \tilde{\sigma}\varepsilon \int_{\Gamma_\varepsilon} \psi_{1,\varepsilon}(x) T_\varepsilon(x) &= - \sum_{i=1}^d \int_{\Omega_\varepsilon} K_\varepsilon(\nabla_y \omega_i + e_i) \cdot \nabla \left( T_\varepsilon \frac{\partial \varphi}{\partial x_i} \right) \\ &\quad - \tilde{\sigma} \sum_{i=1}^d \int_{\Gamma_\varepsilon} (\text{Id} - \mathfrak{J}_\varepsilon) \left( \omega_i \left( \frac{x}{\varepsilon} \right) + \frac{x_i - x_{\varepsilon,k}^i}{\varepsilon} \right) \nabla \frac{\partial \varphi}{\partial x_i}(x) \cdot \frac{(x - x_{\varepsilon,k})}{\varepsilon} T_\varepsilon. \end{aligned} \quad (4.16)$$

Passing to the two-scale limit leads to

$$\begin{aligned} \lim_{\varepsilon \rightarrow 0} \tilde{\sigma}\varepsilon \int_{\Gamma_\varepsilon} \psi_{1,\varepsilon}(x) T_\varepsilon(x) &= - \frac{1}{\text{mes}(Y)} \int_{\Omega} \int_{Y^*} K(\nabla_y \omega_i + e_i) \cdot \left( \nabla \left( T \frac{\partial \varphi}{\partial x_i} \right) + \frac{\partial \varphi}{\partial x_i} \nabla_y T_1 \right) dx \, dy \\ &\quad - \tilde{\sigma} \frac{1}{\text{mes}(Y)} \int_{\Omega} \int_{\Gamma} (\text{Id} - \mathfrak{J})(\omega_i + y_i) y \cdot \nabla \frac{\partial \varphi}{\partial x_i} T \, dy \, dx. \end{aligned} \quad (4.17)$$

In addition to the convergences given in (4.15) and (4.17) we have also the “usual” convergence

$$\lim_{\varepsilon \rightarrow 0} \int_{\Omega_\varepsilon} K \nabla T_\varepsilon \cdot \nabla \varphi_\varepsilon = \frac{1}{\text{mes}(Y)} \sum_{i=1}^d \int_{\Omega} \int_{Y^*} K(\nabla T + \nabla_y T_1) \cdot (\nabla_y \omega_i + e_i) \frac{\partial \varphi}{\partial x_i} \, dx \, dy. \quad (4.18)$$

So taking into account (4.15), (4.17), (4.18) and also the fact that

$$\left| \varepsilon \int_{\Gamma_\varepsilon} \mathcal{O}(\varepsilon) T_\varepsilon \right| \leq C \varepsilon \|T_\varepsilon\|_{H^1(\Omega)} \quad \text{since} \quad \|\mathcal{O}(\varepsilon)\|_{L^\infty(\Omega)} \leq C \varepsilon,$$

the limit of the whole variational formulation is given by

$$\begin{aligned} - \int_{\Omega} \sum_{i,j=1}^d \left[ \int_{Y^*} K(\nabla_y \omega_i + e_i) \cdot e_j + \tilde{\sigma} \int_{\Gamma} (\text{Id} - \mathfrak{J})(\omega_i + y_i) y \cdot e_j \right] e_j \cdot \nabla \frac{\partial \varphi}{\partial x_i} T \, dy \, dx \\ = \text{mes}(Y^*) \int_{\Omega} f \varphi, \end{aligned} \quad (4.19)$$

which is nothing else than an ultra weak variational formulation of the homogenized problem (4.10). We recover the Dirichlet boundary condition for  $T$  because, as the limit of a sequence  $T_\varepsilon$  in  $H_0^1(\Omega)$ , it belongs to  $H_0^1(\Omega)$ . Since (4.10) has a unique solution in  $H_0^1(\Omega)$ , the whole sequence  $T_\varepsilon$  converges to  $T$  and not only a subsequence.  $\square$

**5. Numerical simulations.** In order to show the efficiency of our homogenization approach and to validate it, we perform some numerical simulations for the non linear problem (2.7) in a 2D periodic perforated domain. We use the finite element code CAST3M [10] developed at the French Atomic Energy Commission (CEA). We compare the numerical solution of the “exact” model (2.7) with the “reconstructed” solution of the homogenized model (i.e., including correctors, see below) for smaller and smaller values of  $\varepsilon$ . We evaluate the error in the  $L^2$ -norm for the temperature field and its gradient which allows us to compute numerical rates of convergence for the homogenization process.

Let us note in passing that, in numerical practice, our asymptotic analysis does not follow the usual mathematical procedure (which amounts to let  $\varepsilon$  goes to 0 in a

fixed domain  $\Omega$ ) but rather the following engineering approach. The periodic cells have a fixed unit size and their number goes to infinity which implies that the size of the macroscopic domain goes to infinity like  $\varepsilon^{-1}$ . In other words, we rescale the problem by applying the change of variables  $x \rightarrow x/\varepsilon$ . In any case, this procedure is completely transparent from the point of view of the numerical results presented here.

**5.1. Geometries and meshes.** The geometry corresponds to a cross-section of a typical fuel assembly for a gas-cooled nuclear reactor (see [14] for further references). The unit cell is made of two circular holes in a rectangle (see Figures 5.6, 5.2). Typical meshes of the perforated domain  $\Omega_\varepsilon$  and homogenized domain  $\Omega$  are displayed on Figure 5.1. They correspond to the largest value of  $\varepsilon$ : more periodicity cells will be added for smaller values of  $\varepsilon$ , and each cell will have the same mesh as one cell in Figure 5.1.

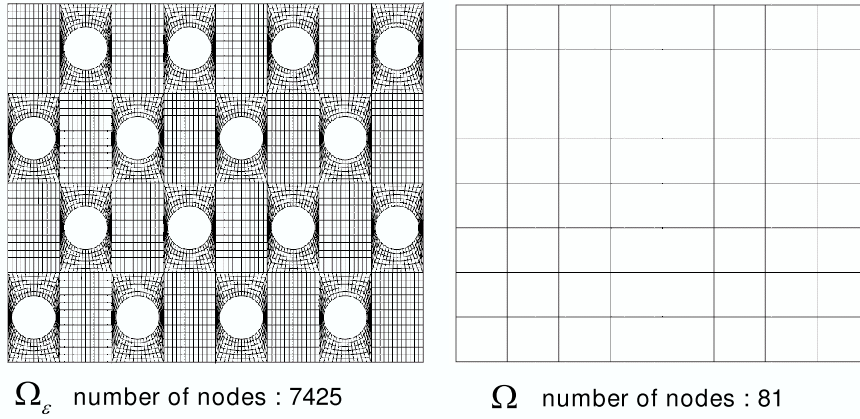


FIGURE 5.1. Initial computational meshes  $\Omega_\varepsilon$  (perforated domain) and  $\Omega$  (solid domain).

**5.2. Computational parameters.** We enforce homogeneous Neumann boundary conditions (adiabatic walls) on the vertical boundaries of  $\Omega_\varepsilon$  and  $\Omega$ , and non homogeneous Dirichlet ones on the horizontal ones. The imposed temperatures are  $T_{sup} = 1300K$  on the upper wall and  $T_{inf} = 600K$  on the lower wall. The conductivity tensor is assumed to be isotropic with conductivity equal to  $30 \text{ W} \cdot \text{m}^{-1} \cdot \text{K}^{-1}$ . The emissivity of the holes boundaries is equal to  $e = 0.8$ . The thermal sources  $f$  and  $g$  are set to zero.

**5.3. Algorithm.** Our numerical computations are done according to the following steps:

1. solve the cell problems (3.3) for a range of macroscopic temperature values  $T$ ,
2. compute a range of homogenized conductivity coefficients  $K_{ij}^*(T^3)$  using the previous cell solutions,

3. solve the nonlinear homogenized problem (3.2) on the non perforated domain  $\Omega$ ; the non-linearity is solved by a fixed-point iterative algorithm,
4. evaluate the fluctuation or corrector term

$$\varepsilon T_1(x, \frac{x}{\varepsilon}) = \varepsilon \sum_{i=1}^2 \frac{\partial T}{\partial x_i}(x) \omega_i \left( T^3(x), \frac{x}{\varepsilon} \right);$$

this step is not straightforward to implement since the result  $T_1$  is defined on the perforated domain mesh while  $T$  lives on the domain mesh and  $\omega_i$  on the cell mesh,

5. reconstruct approximations of the temperature  $T_\varepsilon$  and of the temperature gradient  $\nabla T_\varepsilon$  on the perforated mesh  $\Omega_\varepsilon$ ,  $T(x) + \varepsilon T_1(x, \frac{x}{\varepsilon})$  and  $\nabla T(x) + \nabla_y T_1(x, \frac{x}{\varepsilon})$ , respectively,

6. plot the relative errors  $\text{Err}(T)$  and  $\text{Err}(\nabla T)$  given by

$$\text{Err}(T) = \frac{\|T_\varepsilon(x) - [T(x) + \varepsilon T_1(x, \frac{x}{\varepsilon})]\|_{L^2(\Omega_\varepsilon)}}{\|T(x)\|_{L^2(\Omega)}}, \quad (5.1)$$

$$\text{Err}(\nabla T) = \frac{\|\nabla [T_\varepsilon(x) - T(x) - \varepsilon T_1(x, \frac{x}{\varepsilon})]\|_{L^2(\Omega_\varepsilon)}}{\|\nabla T(x)\|_{L^2(\Omega)}}. \quad (5.2)$$

This procedure is repeated for various values of  $\varepsilon \rightarrow 0$  by using larger and larger meshes.

**5.4. Simulation results and discussion.** We first compute the the solutions of the cell-problem (4.11) for different temperatures:  $T = 0, 1500, 15.E3, 15.E6K$ . Figure 5.2 displays the solutions in the horizontal direction,  $e_1$ , and the vertical direction,  $e_2$ , which are not equivalent by a 90 degrees rotation. In Figure 5.3 we plot the two diagonal components  $K_{11}^*$  and  $K_{22}^*$  of the homogenized conductivity tensor  $K^*$  in terms of the macroscopic temperature in the range 500K to 1500K. Note that these diagonal components have close values so the homogenized medium seems almost isotropic at low temperatures. However, the medium is not isotropic at very high temperatures since the effect of radiation is more important (this will be confirmed below by an asymptotic analysis as  $T$  tends to infinity). Figure 5.4 makes a visual comparison between a numerically converged temperature field  $T_\varepsilon$  (obtained by direct simulation on a fine mesh) and the reconstructed field  $T + \varepsilon T_1$  which is the output of the homogenization process.

In Table 5.4 we display the relative errors on temperature  $\text{Err}(T)$  and  $\text{Err}(\nabla T)$ . On Figure 5.5 we compare these errors with the period  $\varepsilon$  and it squared root  $\sqrt{\varepsilon}$ , respectively. The slopes are in very good agreement. This was theoretically predicted for linear conduction (without radiation): the relative error  $\text{Err}(T)$  behaves like  $\varepsilon$ , while the relative error  $\text{Err}(\nabla T)$  scales like  $\sqrt{\varepsilon}$  (because of boundary layer effects, see [4, 9]).

**5.5. High temperature asymptotic.** As part of the validation process of our homogenization algorithm, it is interesting to study the limit of the cell problems and of the homogenized coefficients when the macroscopic temperature goes to infinity. A formal and simple asymptotic analysis of the cell problems shows that

$$\lim_{T \rightarrow +\infty} \omega_i(T^3, y) = \omega_i^0(y),$$

which leads to a limit of homogenized conductivity given by

$$\lim_{T \rightarrow +\infty} K_{ij}^*(T) = K_{ij}^0 = \int_{Y^*} K(\nabla_y \omega_i^0 + e_i) \cdot (\nabla_y \omega_j^0 + e_j), \quad (5.3)$$

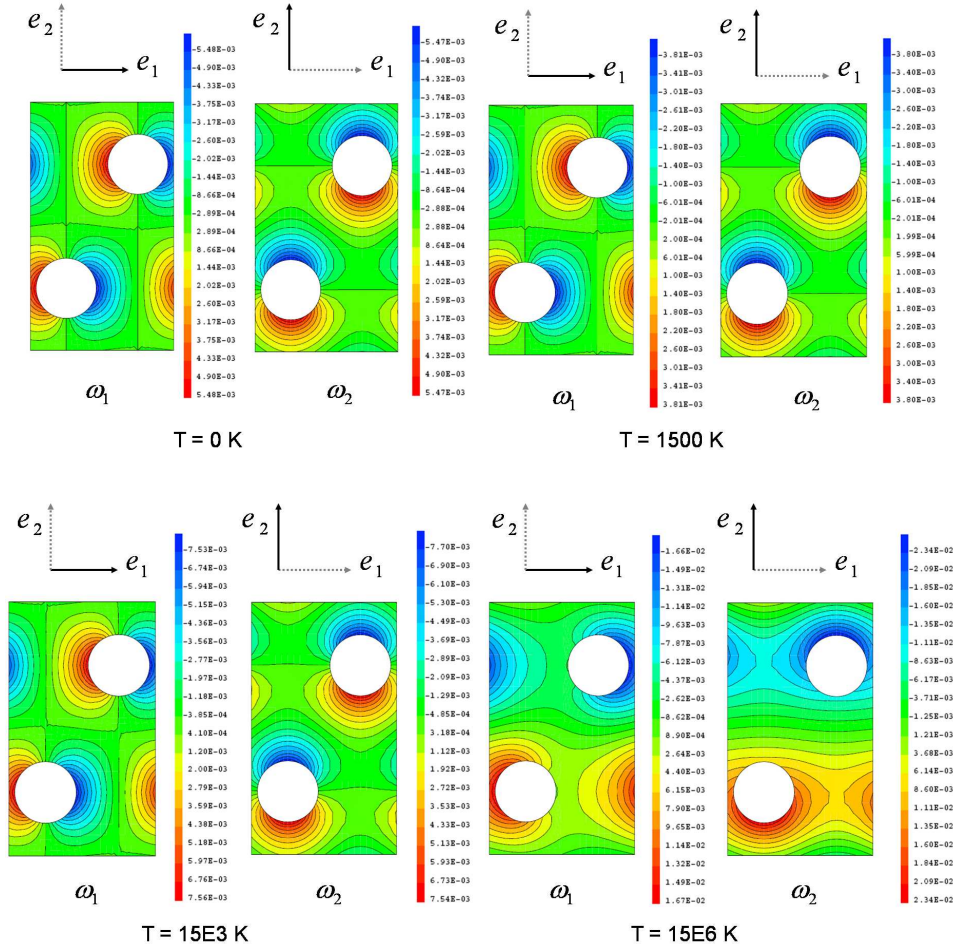


FIGURE 5.2. Cell-problem solutions for increasing temperatures

$N(\varepsilon)$	$\varepsilon$	$\text{Err}(T)$	$\sqrt{\varepsilon}$	$\text{Err}(\nabla T)$
8	$3.5355 \cdot 10^{-1}$	$2.33 \cdot 10^{-3}$	$5.946 \cdot 10^{-1}$	$3.92 \cdot 10^{-2}$
18	$2.357 \cdot 10^{-1}$	$1.32 \cdot 10^{-3}$	$4.854 \cdot 10^{-1}$	$3.15 \cdot 10^{-2}$
32	$1.7678 \cdot 10^{-1}$	$8.88 \cdot 10^{-4}$	$4.204 \cdot 10^{-1}$	$2.41 \cdot 10^{-2}$
72	$1.1785 \cdot 10^{-1}$	$5.22 \cdot 10^{-4}$	$3.432 \cdot 10^{-1}$	$2.20 \cdot 10^{-2}$
98	$1.0102 \cdot 10^{-1}$	$4.26 \cdot 10^{-4}$	$3.178 \cdot 10^{-1}$	$2.03 \cdot 10^{-2}$
128	$8.84 \cdot 10^{-2}$	$3.68 \cdot 10^{-4}$	$2.973 \cdot 10^{-1}$	$1.89 \cdot 10^{-2}$

TABLE 5.1

Relative errors (5.1) and (5.2) in terms of the number  $N(\varepsilon)$  of periodicity cells.

where  $\omega_i^0$ , for  $1 \leq i \leq d$ , are the solutions of cell problems in the limit  $T \rightarrow +\infty$ . It is easily seen that the limit boundary condition is of Dirichlet type, i.e.,

$$\begin{cases} -\text{div}_y(K(e_i + \nabla_y \omega_i^0)) &= 0 & \text{in } Y^*, \\ \omega_i^0 + y_i &= C & \text{on } \Gamma, \end{cases} \quad (5.4)$$

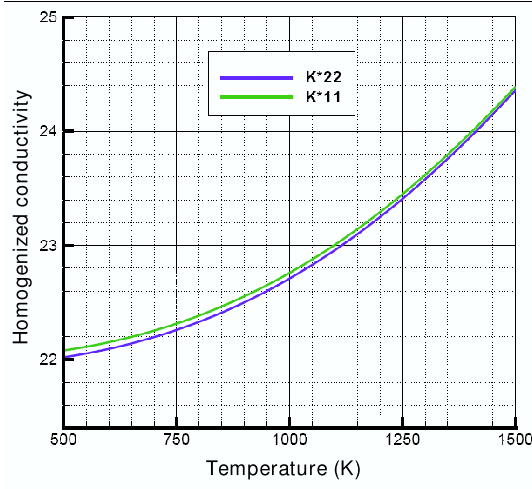


FIGURE 5.3. Diagonal entries  $K_{11}^*$  and  $K_{22}^*$  of the homogenized conductivity tensor

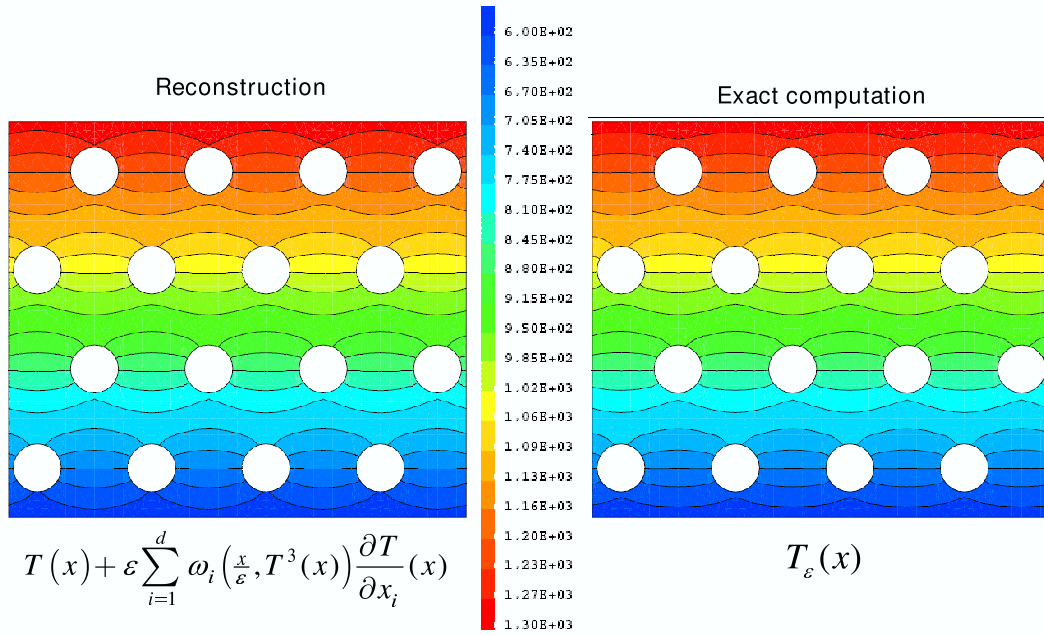


FIGURE 5.4. Comparison between the reconstructed temperature  $T + \varepsilon T_1$  and the direct resolution  $T_\varepsilon$

where  $C$  is any constant (its value does not matter since only the gradient of  $\omega_i^0$  plays a role in the formula for the limit conductivity  $K^0$ ). In Figure 5.6 we plot the two

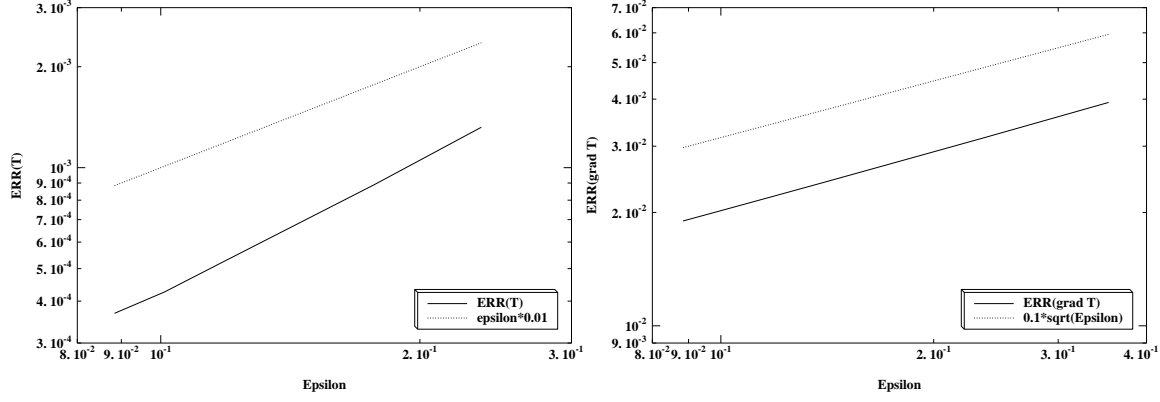


FIGURE 5.5. Convergence of the relative error on the temperature (left) and its gradient (right)

solutions of (5.4) which are indeed very similar to the last line of Figure 5.2. The corresponding limit conductivity is

$$K^0 = \begin{pmatrix} 54.021 & 21.797 \\ 21.797 & 79.217 \end{pmatrix} \quad (5.5)$$

which is highly anisotropic. In Figures 5.7, 5.8 and 5.9 we plot the three different entries of the homogenized conductivity  $K^*$  and check that, for very high temperatures, they reach the theoretically predicted asymptotic behavior (5.3).

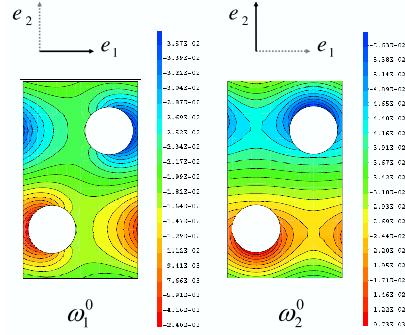
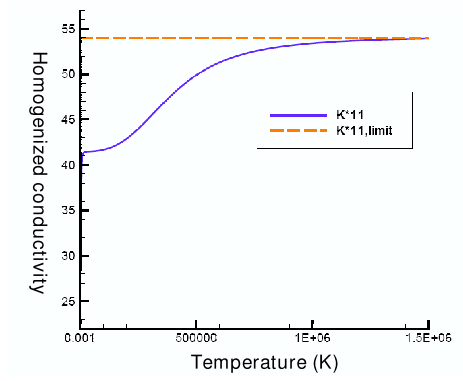
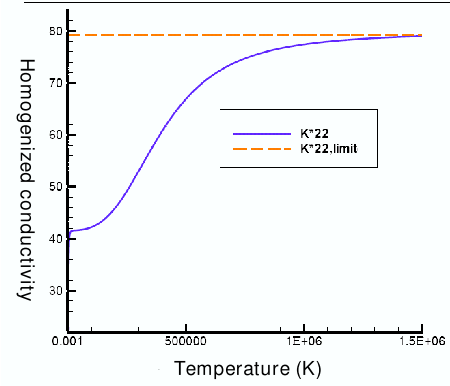
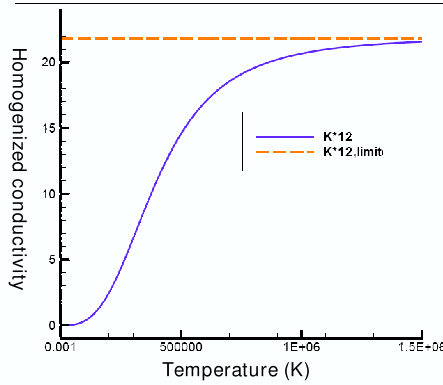


FIGURE 5.6. High-temperature limit of the cell solutions

**6. Conclusion.** We have studied the homogenization of a model of combined conduction and radiative heat transfer problem in a perforated domain. By a formal method of two-scale asymptotic expansions we obtained the homogenized problem which is a non-linear conductivity equation posed in a non-perforated domain. Its homogenized coefficients are computed through a cell problem of linearized radiative heat transfer. We rigorously proved the convergence of the homogenization process by the method of two-scale convergence for a linearization of this model. We exploit the homogenization results to devise a numerical algorithm for the fast computation of approximate reconstructed solutions. This yields a considerable saving in CPU time



FIGURE 5.7. Asymptotic behavior of  $K_{11}^*$ FIGURE 5.8. Asymptotic behavior of  $K_{22}^*$ FIGURE 5.9. Asymptotic behavior of  $K_{12}^*$ 

and memory requirement since only a coarse mesh of the macroscopic domain (and of the unit cell) is required. A numerical validation of our homogenization process has been done for not too small values of  $\varepsilon$ . Of course, our algorithm will be used in practice for much smaller values of  $\varepsilon$ . Future work will concern the coupling of this model with a helium flow model in the channels and with a neutronic diffusion model.

**Acknowledgments.** This research has been supported by the French Atomic Energy Commission (DEN/DM2S at CEA Saclay). The authors thank N. Coulon and A. Stietel for their help.

#### REFERENCES

- [1] G. ALLAIRE, *Homogenization of the Stokes flow in a connected porous medium*, Asymptotic Anal., 2, pp. 203–222, 1989.

- [2] G. ALLAIRE, *Homogenization and two-scale convergence*, SIAM J. Math. Anal., 23(6):1482–1518, 1992.
- [3] G. ALLAIRE, *Shape optimization by the homogenization method*, Applied Mathematical Sciences, vol. 146, Springer-Verlag, New York, 2002.
- [4] G. ALLAIRE AND M. AMAR, *Boundary layer tails in periodic homogenization*, ESAIM Control Optim. Calc. Var., 20(1):209–243, 1999.
- [5] G. ALLAIRE, A. DAMLAMIAN, AND U. HORNUNG, *Two-scale convergence on periodic surfaces and applications*, In Proceedings of the International Conference on Mathematical Modelling of Flow through Porous Media (May 1995), A. Bourgeat et al. eds., World scientific Pub., Singapore (1996).
- [6] G. ALLAIRE AND K. EL-GANAOU, *Homogenization of a conductive and radiative heat transfer problem, Simulation with CAST3M*, In Proceedings of HT2005, ASME Summer Heat Transfer Conference, July 17-22, San Francisco, CA, USA.
- [7] N. BAKHVALOV, *Averaging of the heat transfer process in periodic media in the presence of radiation*, Differential'nye Uravneniya. 17, no. 10, pp. 1765–1773, 1981.
- [8] N. BAKHVALOV AND G. PANASENKO, *Averaging Process in Periodic Media*, Kluwer, Dordrecht, 1989.
- [9] A. BENSOUSSAN, J.L. LIONS, AND G. PAPANICOLAOU, *Asymptotic Analysis for Periodic Structures*, North-Holland, Amsterdam, 1978.
- [10] CAST3M, <http://www-cast3m.cea.fr/cast3m/index.jsp>
- [11] D. CIORANESCU AND P. DONATO, *An Introduction to Homogenization*, 17, Oxford Lecture Series in Mathematics and Applications, Oxford, 1999.
- [12] D. CIORANESCU AND J. SAINT JEAN PAULIN, *Homogenization in open sets with holes*, J. Math. Anal. Appl., 71(2):590–607, 1979.
- [13] M. C. DELFOUR, G. PAYRE AND J.-P. ZOLESIO, *Approximation of Nonlinear Problems Associated with Radiating Bodies in space*, SIAM J. Numer. Anal., 24, no. 5, 1987.
- [14] K. EL GANAOU, *Homogénéisation de modèles de transferts thermiques et radiatifs dans le coeur des réacteurs à caloporteur gaz*, PhD thesis, Ecole Polytechnique, 2006.
- [15] F. P. INCROPERA AND D. P. DEWITT, *Introduction To Heat Transfer*, Wiley, 4th edition, 2001.
- [16] J. -L. LIONS, *Some methods in the mathematical analysis of systems and their control*, Science Press, Beijing, Gordon and Breach, New York, 1981.
- [17] M. F. MODEST, *Radiative Heat Transfer*, McGraw-Hill, New-York, 1993.
- [18] F. MURAT, AND L. TARTAR, *H-convergence*, Topics in the mathematical modelling of composite materials, Progr. Nonlinear Differential Equations Appl., 31, pp. 21–43, Birkhäuser Boston, 1997.
- [19] M. NEUSS-RADU, *Some extensions of two-scale convergence*, Comptes Rendus de l'Académie des Sciences. Série I Mathématique, C. R. Acad. Sci. Paris Sér. I Math, Vol. 322, no. 9, pp. 899–904, 1996.
- [20] G. NGUETSENG, *A general convergence result for a functional related to the theory of homogenization*, SIAM J. Math. Anal., 20(3):608–623, 1989.
- [21] E. SANCHEZ-PALENCIA, *Non-Homogeneous Media and Vibration Theory*, Springer Lecture Notes in Physics, 1980.
- [22] T. TIHONEN, *Stefan-Boltzmann radiation on non-convex surfaces*, Math. Methods Appl. Sci., 20(1):47–57, 1997.